International Journal for Innovative Engineering and Management Research
A Peer Revieved Open Access International Journal
www.ijiemr.org

COPY RIGHT

ELSEVIER SSRN

IJIEMR Transactions, online available on 13th Dec 2019. Link :http://www.ijiemr.org/downloads.php?vol=Volume-08&issue=ISSUE-12

Title APPLICATION OF BOOST CONVERTER TO INCREASE THE SPEED RANGE OF DUAL-STATOR WINDING INDUCTION GENERATOR IN WIND POWER SYSTEMS

Volume 08, Issue 12, Pages: 93-100.

Paper Authors

MRS. SUSHMA SONAWANE , MR. K SUSHARSHAN

Khader Memorial College Of Engineering&Technology,(T.S),INDIA

USE THIS BARCODE TO ACCESS YOUR ONLINE PAPER

To Secure Your Paper As Per UGC Guidelines We Are Providing A Electronic Bar Code

International Journal for Innovative Engineering and Management Research
PEER REVIEWED OPEN ACCESS INTERNATIONAL JOURNAL
www.ijiemr.org

APPLICATION OF BOOST CONVERTER TO INCREASE THE SPEED RANGE OF DUAL-STATOR WINDING INDUCTION GENERATOR IN WIND POWER SYSTEMS

[1]MRS. SUSHMA SONAWANE , [2]MR. K SUSHARSHAN

[1]PG Scholar, Dept of EEE In Khader Memorial College Of Engineering&Technology,(T.S),INDIA.

[2]Associate Professor, Department of EEE in Khader Memorial College Of Engineering&Technology,(T.S),INDIA.

ABSTRACT:

In this paper, a topology using a Dual-stator Winding Induction Generator (DWIG) and a boost converter is proposed for the variable speed wind power application. At low rotor speeds, the generator saturation limits the voltage of the DWIG. Using a boost converter, higher DC voltage can be produced while the DWIG operates at Maximum Power Point Tracking (MPPT) even at low speed and low voltage conditions. Semiconductor Excitation Controller (SEC) of the DWIG utilizes Control-Winding Voltage Oriented Control (CWVOC) method to adjust the voltage, considering V/f characteristics. For the proposed topology, the SEC capacity and the excitation capacitor is optimized by analyzing the SEC reactive current considering wind turbine power-speed curve, V/f strategy, and the generator parameters. The method shows that the per-unit capacity of the SEC can be limited to the inverse of DWIG magnetizing reactance per-unit value. The topology is simulated in MATLAB/Simulink platform and experimented with a scaled 1 kW prototype. Both simulation and experimental results demonstrate wide variable speed operation range of the DWIG and verify the optimization..

Keywords - Boost converter, control-winding voltage oriented control, dual-stator winding induction generator (DWIG), Wind power, Variable speed operation
.

I INTRODUCTION

Wind power is a clean source of energy. It is a "renewable" energy, non-degraded, geographically widespread and mainly seasonal correlation. Moreover, it is an energy that produces no atmospheric emissions or radioactive waste [1, 2]. However, it is random in time and its capture still quite complex. At the beginning, it was exploited in mechanical applications. Thereafter, it has been used to produce electricity. The wind turbine manufacturing technology has been improved during the 1st and 2nd world wars. The oil crisis of 1974 revived again the

International Journal for Innovative Engineering and Management Research
PEER REVIEWED OPEN ACCESS INTERNATIONAL JOURNAL
www.ijiemr.org

studies on the wind turbines. Since the years 1990, the improvement of the technology of the wind turbines made it possible to build aero generators of more than 5 MW [3].

Several technologies are used to capture the energy of the wind (vertical and horizontal axis turbines) and the capture structures are becoming more efficient [4]. Furthermore, the speed of the wind is very important. The integration of wind energy systems requires the reduction of operating costs and maintenance, as well as increasing the power captured from the wind [5]. Many devices exist and, mostly, they use synchronous and asynchronous machines. The control strategies of these machines and their possible network connection interfaces must be able to capture maximum energy over a wider range of variation of wind speeds, to improve the profitability of wind turbines [6]. The studied system here consists of an aero generator three-bladed, with horizontal axis, connected to the network by the dual stator induction generator (DSIG). This type of multiphase machines has some advantages compared to other types of induction machines, such as power segmentation, minimizing torque ripples, reducing the rotor harmonic currents and the use of this machine in wind projects of which powers are of a few MW. It has two fixed three-phase stator windings displaced with an electrical angle α fed by two voltage source inverters [7-9]. By simulating the entire wind conversion chain with different electrical angles, the objective of this work is to define the optimal angle which reduces the total harmonic distortion (THD). In what follows, we perform a quantitative analysis that will give the necessary conclusions about the effect that can have such angle on the reduction of harmonics. A high performance control device requires in general a good response in regulation and must be not very sensitive to the variations of operating conditions and system parameter [10]. Techniques of conventional control of PI type cover a broad range in the industrial applications. These techniques present a simplicity of implementation interest and a facility of the regulators gains synthesis [11].

II. WIND POWER CONVERSION MODELLING

Wind power conversion chain studied includes, besides the DSIG, the inverters 1,2 the DC link voltage, the inverter 3 and the connation to the network through a filter. The inverters 1 and 2 are used to control the speed and flux of the generator. This control is based on the MPPT algorithm. The inverter 3 controls the DC link voltage, the active and the reactive powers exchanged with the network and establishes current to the proper frequency by PI controllers. Fig.1 shows the synoptic scheme of the studied system. Each function of this control device will be detailed.

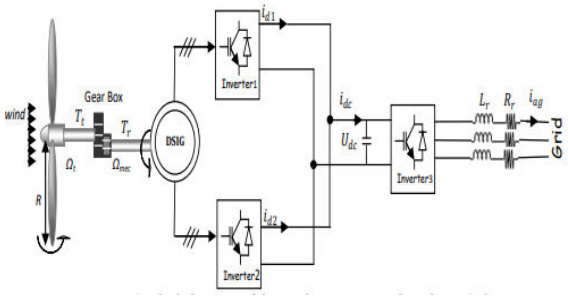

Figure 1. Block diagram of the wind power system based on DSIG.

International Journal for Innovative Engineering and Management Research
PEER REVIEWED OPEN ACCESS INTERNATIONAL JOURNAL
www.ijiemr.org

III WIND TURBINE AND GEARBOX MODELLING

The transmitted power, Pt , captured by the wind turbine, is given by expression (1) [12,13].

$$P_t = 0.5C_p(\lambda)\rho S V^3$$

Where Cpis the power coefficient, S the surface swept by the blades, ρ the air density and V the wind velocity. The torque of the turbine is the ratio of the transmitted power to the shaft speed, Ω . It is given by

$$T_t = \frac{P_t}{\Omega_t}$$

The gearbox adapts the generator to the turbine. The generator torque Tgand the speed Ωtare given by

$$T_g = \frac{T_t}{G} \quad , \Omega_t = \frac{\Omega_{mec}}{G}$$

The mechanical equation can be expressed as:

$$Jp\Omega_{mec} = T_g - T_{em} - f\Omega_{mec}$$

The power coefficient $Cp$is the aerodynamic efficiency of a wind turbine and its evolution is specific to each turbine and wind speed. It depends on the blade pitch angle β and the speed ratio λ which is expressed by [10]:

$$\lambda = \frac{R\Omega_t}{V}$$

Where R is the blade radius.

$$C_p = \left[0.73\left(\frac{151}{\lambda'}\right) - 0.002\beta - 13.2\right] exp\left(\frac{-18.4}{\lambda'}\right)$$

For the valueβ=0, the graph ofCp(λ), given in Fig. 2, is plotted using expression (6).The conversion device extracts a power less than the theoretically recoverable power due to non-zero speed of air masses upstream of the turbine. This presents a theoretical limit called the Betz limit which corresponds to a Cpmax [10,14].

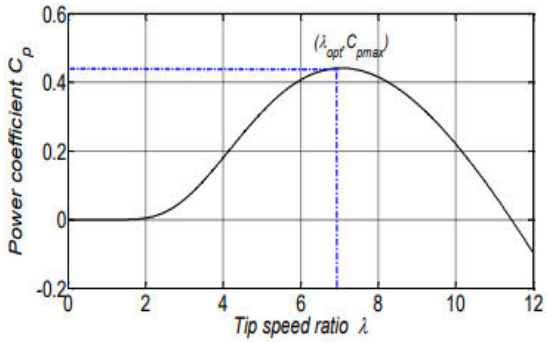

Figure 2. The graph of Cp function .

The maximum power point tracking (MPPT) algorithm permits to maximize the electric power extracted from the wind energy [15]. The tip speed ratio should be kept around its optimal value, λopt. The reference speed $\Omega mec*$ can be written as:

$$\Omega^*_{mec} = \left(\frac{R\lambda_{opt}}{V}\right).G$$

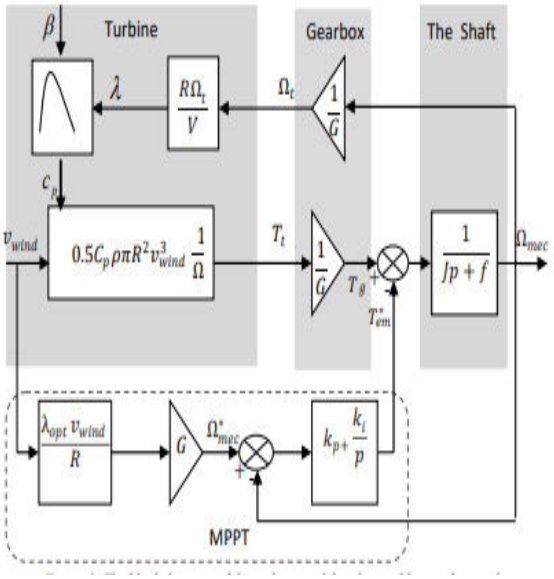

Figure 3. The block diagram of the turbine model with variable speed control.

International Journal for Innovative Engineering and Management Research
PEER REVIEWED OPEN ACCESS INTERNATIONAL JOURNAL
www.ijiemr.org

IV PROPOSED TOPOLOGY

In the wind power application, to ensure that the wind turbine tracks the maximum power point (MPP), variable speed operation is required. Particularly, in low wind speed condition, to increase the output power, the generator must work at low speed, to increase the blade aerodynamic efficiency. This operation increases the annual energy output and decreases the time period of investment return [34]. Fig. 1 shows the wind turbine power-speed curves for various wind speeds in which each curve has its MPP at a specified speed. So, one of the main objectives of the control system is to adjust the generator speed at the optimal value.

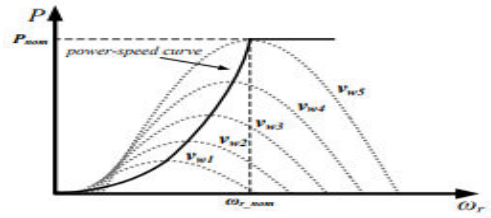

Figure 4. Wind turbine power-speed curve at different wind speeds (vw).

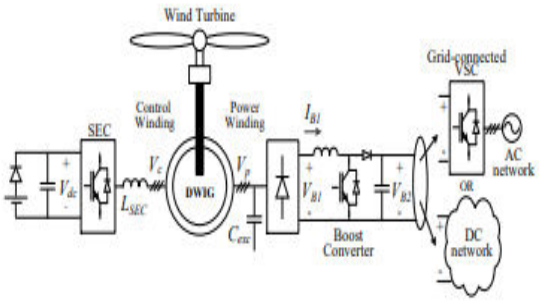

Figure 5. Proposed topology

In the control-winding side, a voltage source converter, named SEC, is connected to the winding via a coupling inductor (LSEC). Also, a low voltage battery with a series diode is connected to DC side of SEC to charge the capacitor for the system start-up. At normal operation, SEC regulates its DClink voltage (Vdc) to a specific reference value, which is more than the battery voltage, so the diode is reverse biased. The main role of SEC is regulation of the control-winding voltage.

V. MODELLING OF THE DSGI

The dual stator induction generator (DSIG) consists of a mobile rotor winding and two fixed three-phase stator windings displaced with an electrical angleα. The windings axes of each star are displaced with an electrical angle $2\pi/3$ and fed by a balanced voltages system, creating a slipping magnetic field in the air-gap. The rotor is a squirrel cage consisting of conducting bars short-circuited by a conductive ring at each end Fig.4 shows schematically the windings of the DSIG. The θr and $(\theta r - \alpha)$angles indicate respectively the rotor position of $as1$phase (star 1) and $as2$ phase (star 2). The quantities relating to the two stars (1 and 2) will be denoted by s1 and s2 respectively [7,8,16].

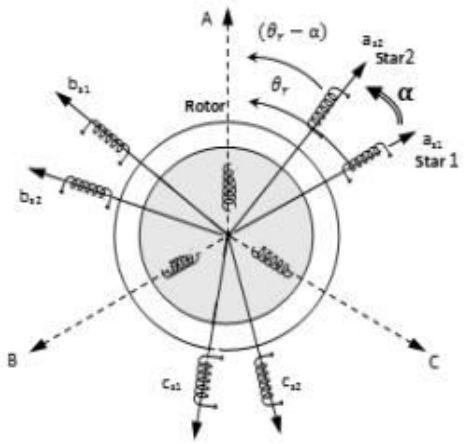

Figure 6. Schematic of dual stator induction generator

International Journal for Innovative Engineering and Management Research
PEER REVIEWED OPEN ACCESS INTERNATIONAL JOURNAL
www.ijiemr.org

The electrical equations in matrix form for the star 1, the star 2 and the rotor are given respectively by:

$$[v_{s1}] = [R_{s1}][[i_{s1}] + \frac{d}{dt}[\varphi_{s1}]$$
$$[v_{s2}] = [R_{s2}][[i_{s2}] + \frac{d}{dt}[\varphi_{s2}]$$
$$[v_r] = [R_r][[i_r] + \frac{d}{dt}[\varphi_r]$$

$$\text{With: } [v_{s1}] = \begin{bmatrix} v_{as1} \\ v_{bs1} \\ v_{cs1} \end{bmatrix}; [v_{s2}] = \begin{bmatrix} v_{as2} \\ v_{bs2} \\ v_{cs2} \end{bmatrix}; [v_r] = \begin{bmatrix} v_{ar} \\ v_{br} \\ v_{cr} \end{bmatrix}$$

The flux expressions (for star1, star 2 and the rotor) in function of the currents are given by:

$$\begin{bmatrix} \varphi_{s1} \\ \varphi_{s2} \\ \varphi_r \end{bmatrix} = \begin{bmatrix} [L_{s1,s1}] & [L_{s1,s2}] & [L_{s1,r}] \\ [L_{s2,s1}] & [L_{s2,s2}] & [L_{s2,r}] \\ [L_{r,s1}] & [L_{r,s2}] & [L_{r,r}] \end{bmatrix} \begin{bmatrix} i_{s1} \\ i_{s1} \\ i_r \end{bmatrix}$$

Where:

$$[L_{s1,s2}] = \begin{bmatrix} L_{ms}\cos(\alpha) & L_{ms}\cos\left(\alpha+\frac{2\pi}{3}\right) & L_{ms}\cos\left(\alpha+\frac{4\pi}{3}\right) \\ L_{ms}\cos\left(\alpha-\frac{2\pi}{3}\right) & L_{ms}\cos(\alpha) & L_{ms}\cos\left(\alpha+\frac{2\pi}{3}\right) \\ L_{ms}\cos\left(\alpha-\frac{4\pi}{3}\right) & L_{ms}\cos\left(\alpha-\frac{2\pi}{3}\right) & L_{ms}\cos(\alpha) \end{bmatrix}$$

$$[L_{s2,r}] = \begin{bmatrix} L_{sr}\cos(\theta_r-\alpha) & L_{sr}\cos(\theta_r-\alpha+\frac{2\pi}{3}) & L_{sr}\cos(\theta_r-\alpha+\frac{4\pi}{3}) \\ L_{sr}\cos(\theta_r-\alpha-\frac{2\pi}{3}) & L_{sr}\cos(\theta_r-\alpha) & L_{sr}\cos(\theta_r-\alpha+\frac{2\pi}{3}) \\ L_{sr}\cos(\theta_r-\alpha-\frac{4\pi}{3}) & L_{sr}\cos(\theta_r-\alpha-\frac{2\pi}{3}) & L_{sr}\cos(\theta_r-\alpha) \end{bmatrix}$$

$$\begin{bmatrix} \varphi_{s1} \\ \varphi_{s2} \\ \varphi_r \end{bmatrix} = \begin{bmatrix} [L_{s1,s1}] & [L_{s1,s2}] & [L_{s1,r}] \\ [L_{s2,s1}] & [L_{s2,s2}] & [L_{s2,r}] \\ [L_{r,s1}] & [L_{r,s2}] & [L_{r,r}] \end{bmatrix} \begin{bmatrix} i_{s1} \\ i_{s1} \\ i_r \end{bmatrix}$$

Where:

$$[L_{s1,s2}] = \begin{bmatrix} L_{ms}\cos(\alpha) & L_{ms}\cos\left(\alpha+\frac{2\pi}{3}\right) & L_{ms}\cos\left(\alpha+\frac{4\pi}{3}\right) \\ L_{ms}\cos\left(\alpha-\frac{2\pi}{3}\right) & L_{ms}\cos(\alpha) & L_{ms}\cos\left(\alpha+\frac{2\pi}{3}\right) \\ L_{ms}\cos\left(\alpha-\frac{4\pi}{3}\right) & L_{ms}\cos\left(\alpha-\frac{2\pi}{3}\right) & L_{ms}\cos(\alpha) \end{bmatrix}$$

$$[L_{s2,r}] = \begin{bmatrix} L_{sr}\cos(\theta_r-\alpha) & L_{sr}\cos(\theta_r-\alpha+\frac{2\pi}{3}) & L_{sr}\cos(\theta_r-\alpha+\frac{4\pi}{3}) \\ L_{sr}\cos(\theta_r-\alpha-\frac{2\pi}{3}) & L_{sr}\cos(\theta_r-\alpha) & L_{sr}\cos(\theta_r-\alpha+\frac{2\pi}{3}) \\ L_{sr}\cos(\theta_r-\alpha-\frac{4\pi}{3}) & L_{sr}\cos(\theta_r-\alpha-\frac{2\pi}{3}) & L_{sr}\cos(\theta_r-\alpha) \end{bmatrix}$$

The mathematical model of the DSIG is derived from the PARK theory in order to simplify the differential equations as shown in Fig

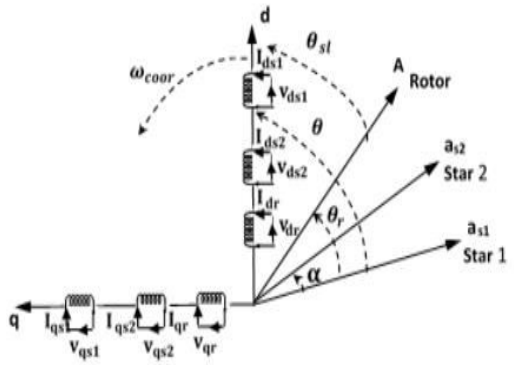

Figure 7. Representation of the DSIG model along the axes (d, q)

$$[\dot{I}] = [L]^{-1}\{[B][U] - \omega_{gl}[C][I] - [D][I]\}$$

Where:

$$\omega_{gl} = \omega_s - \omega_r \ , \ \omega_r = p * \Omega_{mec}$$
$$[U] = [v_{ds1}v_{qs1}v_{ds2}v_{qs2}v_{dr}\ v_{qr}]^t$$
$$[I] = [i_{ds1}i_{qs1}\ i_{ds2}\ i_{qs2}\ \ i_{dr}\ i_{qr}]^t$$
$$[\dot{I}] = \frac{d}{dt}[I]$$
$$[B] = diag\,[1\ 1\ 1\ 1\ 0\ 0]$$

$$[C] = \begin{bmatrix} 0 & 0 & 0 & 0 & 0 & 0 \\ 0 & 0 & 0 & 0 & 0 & 0 \\ 0 & 0 & 0 & 0 & 0 & 0 \\ 0 & 0 & 0 & 0 & 0 & 0 \\ 0 & -L_m & 0 & -L_m & 0 & -(L_r+L_m) \\ L_m & 0 & L_m & 0 & L_r+L_m & 0 \end{bmatrix}$$

$$[L] = \begin{bmatrix} (L_{s1}+L_m) & 0 & L_m & 0 & L_m & 0 \\ 0 & (L_{s1}+L_m) & 0 & L_m & 0 & L_m \\ L_m & 0 & (L_{s2}+L_m) & 0 & L_m & 0 \\ 0 & L_m & 0 & (L_{s2}+L_m) & 0 & L_m \\ L_m & 0 & L_m & 0 & (L_r+L_m) & 0 \\ 0 & L_m & 0 & L_m & 0 & (L_r+L_m) \end{bmatrix}$$

$$[D] = \begin{bmatrix} R_{s1} & -\omega_s(L_{s1}+L_m) & 0 & -\omega_s L_m & 0 & -\omega_s L_m \\ \omega_s(L_{s1}+L_m) & R_{s1} & \omega_s L_m & 0 & \omega_s L_m & 0 \\ 0 & -\omega_s L_m & R_{s2} & -\omega_s(L_{s2}+L_m) & 0 & -\omega_s L_m \\ \omega_s L_m & 0 & \omega_s(L_{s2}+L_m) & R_{s2} & \omega_s L_m & 0 \\ 0 & 0 & 0 & 0 & R_r & 0 \\ 0 & 0 & 0 & 0 & 0 & R_r \end{bmatrix}$$

The electromagnetic torque is expressed by:

$$T_{em} = P\frac{L_m}{(L_m+L_r)}[(i_{qs1}+i_{qs2})\varphi_{dr} - (i_{ds1}+i_{ds2})\varphi_{qr}]$$

The active and reactive power are described by:

$$\begin{cases} P_s = v_{ds1}i_{ds1} + v_{qs1}i_{qs1} + v_{ds2}i_{ds2} + v_{qs2}i_{qs2} \\ Q_s = v_{qs1}i_{ds1} - v_{ds1}i_{qs1} + v_{qs2}i_{ds2} - v_{ds2}i_{qs2} \end{cases}$$

BOOST CONVERTER MPPT CONTROL

As the excitation control regulates the DWIG voltages, the boost converter controls the generator active power based on MPPT. The boost converter provides a wide speed range of operation, including low-speed condition, where the DWIG voltage is reduced according to V/f strategy. Boost

International Journal for Innovative Engineering and Management Research
PEER REVIEWED OPEN ACCESS INTERNATIONAL JOURNAL
www.ijiemr.org

converter accommodates the increase in the output voltage and connects the generator to a higher voltage level. For MPPT, the control strategy presented in [32] is employed. The control scheme for the boost converter is shown in Fig.

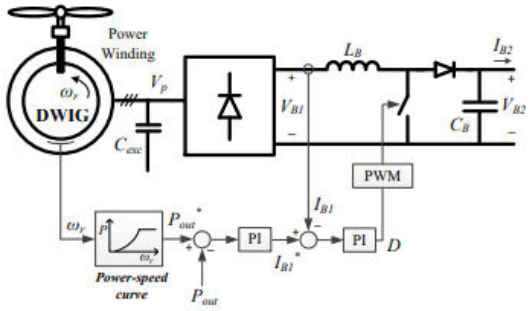

Figure 8. Boost Control strategy for MPPT operation.

To achieve MPPT, the controller uses a look-up table, which is obtained from the power-speed curves presented in Fig. 1. In the look-up table, for any given DWIG speed (ωr), the optimum power (Pout *) is stored.

$$P_{out} = V_{B2} I_{B2} = V_{B1} I_{B1}$$

VB1 can be written as a constant ratio of power-winding voltage if the diode rectifier voltage drop is ignored. Since the DWIG control and power windings experience the same air gap flux, controlling the voltage of control-winding leads to regulation of power-winding voltage. Therefore, the power winding voltage can be replaced by the control-winding voltage considering the voltage drop across the generator impedance.

$$V_{B1} = \frac{3\sqrt{2}}{\pi} . U_p = \frac{3\sqrt{2}}{\pi} . \frac{n_p}{n_c} . U_c - \Delta U(I_{B1}, U_c)$$

$$P_{out} = \left(\frac{3\sqrt{2}}{\pi} . \frac{n_p}{n_c} . U_c - \Delta U(I_{B1}, U_c) \right) . I_{B1}$$

Where Up and Uc denote the line voltage of power-winding and control-winding respectively; ΔU is the voltage drop across control-winding and power-winding; np/nc is the turn ratio of the windings. Since Uc is regulated by the excitation control to its reference value, Pout - given in (13)- can be controlled by IB1. So in the power regulation loop, Pout is compared with its reference value and using a PI controller, the reference value of IB1 is obtained. In the current regulation loop, IB1 is compared with its reference value and the output error is passed through another PI controller to determine the duty cycle (D) of the boost converter. Finally, using PWM technique with saw-tooth carrier waveform, the duty cycle is converted to the switch drive signal.

VI.RESULTS

Using MATLAB/Simulink organize, DWIG system is reproduced to evaluate its display and concentrate the effect of perfect excitation capacitor. Amusement results are gotten for the 2.3MW DWIG structure displayed in fragment V. In the system, the lift converter yield is related with the network by methods for a 3-pahase voltage source converter. Cexc is set to 0.15 p.u., as obtained in the past territory.

International Journal for Innovative Engineering and Management Research
PEER REVIEWED OPEN ACCESS INTERNATIONAL JOURNAL
www.ijiemr.org

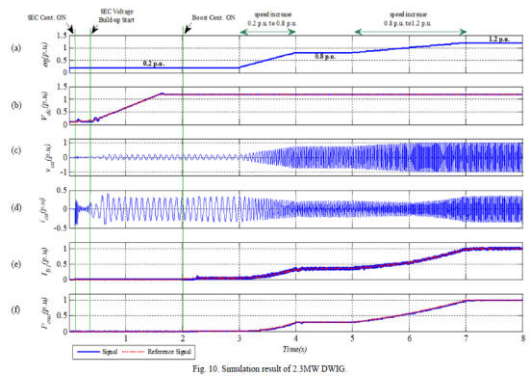

Fig. 10. Simulation result of 2.3MW DWIG.

Figure 9: shows the entertainment eventual outcome of the DWIG structure. At t = 0.1 s,

VII.CONCLUSION

This paper proposes a topology for variable speed wind control application using twofold stator-winding acknowledgment generator. A lift converter is utilized for MPPT and wide range variable speed movement, especially at low-speed condition is obtained. At low speeds, DWIG voltage is dropped in light of V/f philosophy and a lift converter is used to extend the voltage level to meet the higher and relentless voltage essential, for instance, in voltage source converter DC link or toward the ocean DC sort out applications. In the proposed topology, by picking the perfect excitation capacitor, the point of confinement of the semiconductor excitation controller is restricted. Finally, to check the right movement of the proposed system, amusement and test outcomes are presented which support the wide-speed broaden action of the structure and the excitation capacitor improvement procedure.

VIII. REFERENCES

[1] REN21, "Renewables 2016: Global status report," 2016. [Online]. Open: http://www.ren21.net.

[2] F. Blaabjerg and K. Mother, "Future on Power Electronics for Wind Turbine Systems," IEEE Journal of Emerging and Selected Topics in Power Electronics, vol. 1, no. 3, pp. 139-152, Sept. 2013.

[3] Z. Chen, J. M. Guerrero, and F. Blaabjerg, "A Review of the State of the Art of Power Electronics for Wind Turbines," IEEE Transactions on Power Electronics, vol. 24, no. 8, pp. 1859-1875, Aug. 2009.

[4] V. Yaramasu, B. Wu, P. C. Sen, S. Kouro and M. Narimani, "Highpower wind essentialness change systems: State-of-the-craftsmanship and creating advancements," Proceedings of the IEEE, vol. 103, no. 5, pp. 740-788, May 2015.

[5] H. Nian and Y. Tune, "Direct Power Control of Doubly Fed Induction Generator Under Distorted Grid Voltage," IEEE Transactions on Power Electronics, vol. 29, no. 2, pp. 894-905, Feb. 2014.

[6] H. Li, and Z. Chen, "Outline of different breeze generator systems and their assessments," IET Renew. Power Gener., vol. 2, no. 2, pp. 123-138, Jun. 2008.

[7] S. M. Muyeen, R. Takahashi, and J. Tamura, "Action and Control of HVDC-Connected Offshore Wind Farm," IEEE Transactions on Sustainable Energy, vol. 1, no. 1, pp. 30-37, April 2010.

[8] N.M. Kirby, L. Xu, M. Luckett, and W. Siepmann, "HVDC transmission for huge toward the ocean wind farms," Power Eng. J., vol. 16, no. 3, pp. 135-141, Jun. 2002.

[9] A. Egea-Alvarez, F. Bianchi, A. Junyent-Ferre, G. Gross, and O. GomisBellmunt, "Voltage Control of Multiterminal VSC-HVDC Transmission Systems for Offshore Wind Power Plants: Design and

Implementation in a Scaled Platform," IEEE Trans. Ind. Electron., vol. 60, no. 6, pp. 2381-2391, Jun. 2013.